EFDA–JET–CP(11)01/06

Ph. Mertens and JET EFDA contributors

Detailed Design of a Solid Tungsten Divertor Row for JET in Relation to the Physics Goals

Detailed Design of a Solid Tungsten Divertor Row for JET in Relation to the Physics Goals

Ph. Mertens and JET EFDA contributors*

JET-EFDA, Culham Science Centre, OX14 3DB, Abingdon, UK

Institute of Energy and Climate Research IEK-4 – Plasma Physics, Forschungszentrum Jülich GmbH, Association EURATOM-FZJ, Partner in the Trilateral Euregio Cluster, D-52425 Jülich, Germany
** See annex of F. Romanelli et al, "Overview of JET Results", (23rd IAEA Fusion Energy Conference, Daejon, Republic of Korea (2010)).*

Preprint of Paper to be submitted for publication in Proceedings of the
13th International Workshop on Plasma-Facing Materials and Components for Fusion Applications
Rosenheim, Germany
(9th May 2011 - 13th May 2011)

ABSTRACT

In the frame of the ITER-like Wall (ILW) for the JET tokamak, a divertor row made of bulk tungsten material was developed for the position where the outer strike point is located in most of the foreseen plasma configurations. In the absence of active cooling this represents a formidable challenge: such plasma-facing components are fully metallic and subject to much higher electromagnetic loads than commonly encountered. The basic geometry of the divertor is similar to the previous one, made of carbon-fibre composite. The present contribution stresses the wide span of different aspects that contributed to the conceptual and detailed developments, in relation to the physics goals. They are presented with emphasis on the results of thermal and electromagnetic models and of their validation in electron (JUDITH-2) and ion-beam (MARION) facilities. Several operational constraints arise from the absence of active cooling and from the segmentation; it will force the exploitation to be driven by this Plasma-Facing Component (PFC) to a large extent. Recommended scenarios encompass sweeping procedures over several thermally isolated stacks and an energy deposition below 60MJ/m^2 which can be obtained with impurity seeding Significant progress in the preparation of PFC-compatible divertor plasma was achieved in the last physics campaign before shutdown.

1. INTRODUCTION

A bulk tungsten divertor row was developed for the outer divertor in the JET tokamak, in the frame of the ITER-like Wall project (ILW[1]). The selected design not only accounts for inescapable boundary conditions but also considers the compromises in terms of physics needs and expectations. The bulk tungsten modules are located at the outer strike point for the majority of scenarios aimed at, in particular with medium of high triangularity shapes. The high power fluxes, in the order of 7MW/m^2 for 9s, come on top of the main requirements: a high rate of change of the magnetic field ($\partial B/\partial t \leq 100$T/s during the worst case disruption at high plasma current) and the absence of any active cooling within technical reach. The consequences and usable range of parameters are elaborated on in the following. An overview of operational limits for the ILW was given in [2]. The current status of the ITER-like Wall project is presented in [3] together with the main lines of the experimental programme. The question of limits has a strong link to scenario development and programme goals. Progress made in the development of feasible plasma scenarios is reported in [4,5,6,7, 8].

The present article is organised in a top to bottom structure with respect to the actual physical modules, considering in sequence the plasma-facing tungsten tile followed by the supporting structure, a main carrier interfaced to the tile above by the clamping arrangement, and to the torus base plate below by an ad hoc adaptor. This thread also corresponds to the development history: as a conceptual design for the tile was found, it became clear that a new carrier was required and, later on, the new carrier called for a completely redesigned adaptor to the given mounting surface (the JET so-called base carrier). The electromagnetic analysis [9] was steadily accompanying all these steps as a potentially critical issue. Implications and relations to the physics goals are discussed at each stage. It is clear that the main aim was to mimic the former 3D-shaped, unsegmented tiles made of Carbon-Fibre Composite (CFC) and attempt to get close to their performance, a formidable

challenge in view of the mentioned boundary conditions and of the not so adequate material properties of tungsten. The reader interested in this statement may be referred to [10,11,12] on the technical side or [13,14] on the plasma physics side. The hardware is described in detail in [15] which gives an overview and in [16] which deals with the clamping scheme.

2. THE TUNGSTEN TILE

2.1 DIMENSIONS

For thermo-mechanical as well as electromagnetic reasons, the plasma-facing tungsten tile has to be segmented in both toroidal and poloidal directions. Each tile (96 of them in total, distributed in 48 modules) consists of four stacks of 24 tungsten blades each. The dimensions of these lamellae were determined from engineering considerations. The height of 40mm derives from the highest acceptable gradient of $\partial T/\partial z \leq 5 \cdot 10^4$ K/m with an upper tungsten surface which can attain the nominal value of $T_{W,surf}$ =2200°C within seconds and a contact pad at the bottom still around $T_{W,init}$ = 200°C. The poloidal extension is of about 60 mm, a sensible value to keep internal stresses within bounds during the thermal expansion (see [16] and below). The thickness of a lamella, in toroidal direction, was deliberately set to ~6mm from similar considerations and practicability of the manufacturing process qualification. The deformation of single lamellae in poloidal direction is shown in Fig.2. It is by no means negligible in the design.

Note that these dimensions, together with the toroidal gap width of 1 mm and the dimensions of the tile, determine the total minimum amount of tungsten, around 2100kg. Through the sheer heat capacity, the necessary cooling time $\Delta t_{cooling}$ = 2700-3600s for most cases with energy depositions in the range 20-50MJ/m^2 [(1)]. The main factors that can be used to modify this cooling time are the initial bulk temperature and, for a given energy density, the pulse length as well as the strike point sweep (see below). The power handling is conveniently specified in the form of a tolerable energy density for reasonably similar high-heat-flux plateaus (5-10s). But the detailed time evolution of the energy deposition must be considered – especially for short pulses – to assess the maximal $T_{W,surf}$ temperature, hence the radiative losses from the plasma-facing surface, a substantial contribution to the cooling process at high temperatures where the emissivity of tungsten is more favourable: we assume a variable emissivity with $\varepsilon_W \leq 0.28$ at the high end.

2.2 MATERIAL STRENGTH

The tungsten grade was specified as the highest feasible with respect to the material properties and deliverable amount to a purity of 99.95%. The tensile mechanical properties – an initially expected yield strength $R_{p0.2}$ > 175MPa at 1500°C or the ultimate tensile strength according to membrane specifications – are not the most important parameters (the proof stress was later specified to the more easily controllable temperature of 500°C): in view of the totally unavoidable temperature excursions during plasma operation owing to steady state and transients, a specification of the material ductility is more relevant, namely with the lowest possible Ductile-to-Brittle Transition Temperature (DBTT). At the other end of the temperature range, re-crystallisation occurs, the reason for the three step

[(1)] *the shortest cooling time does not necessarily correspond one-to-one to the lowest deposited energy.*

approach to the allowed tile temperature of $T_{W,surf\text{-}max.}$ = {1200°C, 1600°C, 2200°C} in sequence to avoid an early degradation of the material. Both aspects of the temperature cycling, DBTT at the low end and re-crystallisation at the high end, were explained in [16]. It is also shown therein that the main drawback of the absence of active cooling with respect to the bulk tungsten, and ultimately the most probable cause of material failure, is the evolution of material properties to a local exhaustion of ductility. To minimise the consequences, it was decided that tungsten should, to the largest extent, be acted upon in compression only.

2.3 PHYSICS

The gap width between lamellae in a stack is specified to 1 mm and achieved through accurate manufacturing within ±10μm typically. From the technical point of view, a twodimensional profile could be cut for the wetted facet, which is kept unchanged over the full lamella length (Fig.3). On the plasma side, the incidence of the field lines is defined by an azimuthal angle $\theta_{||}$ and an elevation $\theta_{\perp}$ with respect to the plasma-facing surface; the interested reader can consult [17] for definitions. The elevation depends on the major radius, so we usually consider typical values for the third tungsten stack from top (from the high field side, stack (3) in Fig.1), a convenient position for the outer strike point. In terms of local shadowing, the tolerable $\theta_{\perp}$ values roughly lie in the range (0°–7.0°). Although, at the high range of $\theta_{\perp}$, low values for the safety factor $q_{95} > 2.3$ should be allowed, the design was optimised for shallow θ angles, especially elevations of the order of 1°. Much steeper angles of incidence were used in the exposure of reference stacks to an ion and electron beam in the MARION facility [18]. Figure 4 shows an infrared view of the tungsten surface after exposure under $\theta_{\perp}$ = 6.7°. The geometrical enhancement of the heat flux [20] is clearly seen as a region of higher temperature on each lamella.

The effective global shadowing between different stacks is obtained through chamfering or tilt of the individual stacks [19]. The achieved result obviously depends on manufacturing and installation tolerances and on the possibly reduced vertical steps between successive stacks. As can be seen on Fig.1, the shadowing between stacks is also ensured in poloidal direction: the steps down from the High Field Side (HFS) to the Low Field Side (LFS) are noticeable. The segmented tile aims in this way at covering an allowable domain for the ($\theta_{||}$,$\theta_{\perp}$) couple that is not too far from the former CFC tile performance. The power handling capabilities are discussed in section 4. Physical sputtering of tungsten and the attainable level of triangularity in the divertor considered shall be left outside the scope of this paper: bulk material renders the former question null and void and the developers had no influence on the latter since the geometry was given.

3. THE CARRIER

3.1 THE INCONEL WEDGE

The tile supporting structure is entirely new, mainly for electromagnetic reasons. It consists in an Inconel wedge with eight “wings” which extend in toroidal direction. Each wing supports a stack of tungsten lamellae. The wedge carrier is deeply cut in all directions between these wings (Fig.5a)

to minimise the electromagnetic forces that result from high rates of change of the magnetic field [9]. The wedge carrier is pre-loaded, which means bent upon tightening of the fastening bolts to the underlying adapter. Obtaining the correct tile height within 0.3mm to ensure adequate shadowing properties when installed is by no means straightforward. Moreover, the lamella-to-lamella deviation could not exceed ±50μm. This is the reason why a survey of the main gaps between different modules, that is between different carriers, was carried out after installation in the JET torus with a noncontact laser gauge (Gap Gun [21], 40mm wide head). All measured vertical steps appear to be within the requested tolerance.

A limiting feature of the wedge carrier is the maximum temperature that can be reached at the contact to the lamellae feet: the tolerable temperature was deliberately fixed to $T_{Inc,max.} = 600°C$ owing to the steep degradation of the mechanical properties of the selected Inconel alloy 625 above this value. The contact pads of the tungsten tile are not directly in contact with the wedge wings. A molybdenum foil is inserted in between. Nevertheless, the insulation does not make much difference during the long cooling phase and the temperature of the carrier has to be carefully monitored.

3.2 TILE CLAMPING

The clamping scheme is extensively described in [16]. Its complexity comes in the first place from the unknown adequacy of the tungsten material for plasma-facing components that are subject to thermal cycling over wide temperature domains. But also from the integral heat flux of up to 60-70MJ/m^2 and from the necessity to resists the mentioned loads generated by disruptions. And finally from the very low coefficient of thermal expansion below or around $\alpha_W \approx 5 \cdot 10^{-6}$ /K in the temperature range of interest, a coefficient of thermal expansion which cannot be matched easily by usual structure materials as is well known. The constraint of compression (section 2.2) arises from the relative weakness of tungsten with respect to tensile stresses when it is subject to extreme temperatures at both ends of the operating range.

Incidentally, a good way to proceed might be to bolt down the tungsten tile as strongly as possible to an hypothetic carrier that could be in turn hardly tightened to the base carrier. This turned out to be unrealistic in the present case, if only because of historical reasons which have determined the given configuration of the interface.

Again, possible limitations as far as the physics is concerned deal with the energy deposition. They are due to the maximum allowable temperature for the clamping, precisely for the incorporated spring elements in the form of spring discs: $T_{springs,max.} = 330°C$ to avoid excessive creep and settling [22]. The spring discs are thermally insulated from the highest temperature in the clamping – the temperature of a Densamet [23] rail embedded in the carrier wing – by a pile of Inconel shims. An exploded view of the clamping is given in Fig.5b.

3.3 ADAPTOR

A star shaped adaptor was developed to fit to the wedge carrier and, at the same time, to match the existing configuration of possible fixings in the base carrier plate. It thus acts as a plain interface

between the tungsten tile carrier and the CFC base in the torus.

Furthermore, it withstands the electromagnetic loads and bears all required Remote Handling (RH) features, as do all other components in the present design. The adaptor is seen in place on Fig.1. As the adaptor does not directly influence the boundary conditions to the physics of the plasma scenarios, it will not be discussed further in the present article.

In summary, the following engineering limits were defined in terms of temperatures of the different components:

$T_{W,surf\text{-}max.}$ = {1200°C, 1600°C, 2200°C} for the tungsten, in three sequential steps;
$T_{Inc,max.}$ = 600°C for the Inconel 625 carrier (wedge); and
$T_{springs,max.}$ = 330°C for the clamping springs.

The following section shows how these transform to specifications for the deposited energy density.

4. HIGH HEAT FLUX TESTS

First high heat flux tests took place in the electron beam JUDITH-2 facility during the conceptual phase [24,25]. For a limited number of pulses, *O*(100), the tungsten surfaces displayed a low level of damage up to exposures around 9MW/m^2 for more than 10s. However, the infrastructure of that very first design suffered from peak temperatures above 700°C that could be imputed to an excessive compactness and to the penetration of the electron beam in the gaps, down to the molybdenum spacers, owing to the high angle of incidence $\theta_\perp$~80°. In a second phase, two prototypes were exposed to an ion and neutral beam in MARION, the NBI test bed [k] for the neutral injectors of the TEXTOR tokamak [26]: one prototype was a standard Stack No.3 (third from the HFS side, see Fig.1) and the other one represented the shallow stack No.4 (outermost stack to the LFS). A special scraper was designed to reduce the beam height to a usable slit of only 20 mm to allow bombardment under a realistic angle $\theta_\perp$ of 5-7°.

4.1 EXPERIMENTAL RESULTS

These tests have been reported on in several publications, especially in [u]. On account of the beam profile, the deposited power is flat within ± 10% over the stack width but under a wetted fraction of 0.7 ($\theta_\perp$ = 6.7°), the power density drops by 50% to the far end in toroidal direction (along the beam axis).

The highest energy density which can be deposited amounts to $E_{dep} < 60MJ/m^2$ [+0%/–10%] over the wetted area. One of the main limiting factors is the temperature of the wedge carrier at the contact with the tungsten tile which should not exceed 600°C (section 3). The other ones are the temperature on top of the vulnerable pile of spring discs and, depending on how far the test should go, the highest temperature of the tungsten tile – a matter of adjustable power density for a given amount of deposited energy. The latter never exceeded 2000°C during the experimental tests, with an energy deposition that was close to uniform.

A 3CCD camera view of the second prototype in the visible range is given in Fig.6 during

a MARION pulse. The spectral range obviously exaggerates the deviations between hotter and colder regions of the tungsten surface. But at the same time, it gives a striking impression of the effect of lamella misalignments. The prototype was aligned with the same precision as the actual divertor row.

4.2 COMPARISON TO MODELS AND IMPLICATIONS

From the engineering point of view, the tungsten tile was initially developed under consideration of an absolutely uniform power deposition. In a second step the local wetted fraction (shadowing between consecutive lamellae) and the global wetted fraction (shadowing between neighbouring stacks) were duly taken into account [27]. Finally, poloidal profiles of the power deposition were assumed according to

$$q\,(MWm^{-2}) \sim \frac{1}{\lambda_m}\,\frac{B_{\phi,m}}{B_{p,m}}\,\frac{1}{2\pi\,R_{str}}\,\frac{\sin(\alpha+\theta_\perp)}{\cos\theta_\perp}\,\exp\left(\frac{-a\,(R-R_{str})}{\lambda_m}\,\frac{B_{\phi,m}}{B_{p,m}}\,\tan\theta_\perp\right) \qquad (2)$$

With λ_m, the mid-plane decay length (~5mm); (B_θ, B_p) the toroidal and radial field strengths; R_{str}, the position of the strike point; and a, a fixed positive value. Fig.7a,b make the comparison possible. Details can be found in [17].

Largest deviations of 7b-7d to the uniform case lie in the local temperature $T_{W,surf\text{-}max}$ which can substantially differ from the average value. This effect influences the tungsten lifetime which could become significantly shorter and the cooling which is accelerated by the radiative contribution from the tile surface at high temperatures. For a given integral amount of deposited energy, short time intervals i.e. high power densities are less favourable for the tungsten material but beneficial for the radiative losses and consequently beneficial too for the supporting structure (tile clamping and wedge carrier).

Sweeping of the strike point position is a major tool to control this effect as discussed in [17], and avoid overheating of the tile. An energy of ~150MJ (100%) can presumably be deposited by appropriate sweeps over three stacks. The model shows that it is indeed possible over stacks No. 2-3-4 in proportion 20:40:36 with 4% left in the long outer tail of the profile over the tungsten coated tile 6 of the outer divertor. The energy densities and energies mentioned here above all refer to integral values over the complete plasma pulse. ELMs were not considered so far, except through the fact that their energy contributes to the full amount of deposited energy. On the one side, they can significantly increase the temperature of the plasma-facing surface, but on the other side this effect is possibly alleviated by a broadening of the footprint [28]. With a melting threshold of ~50MW m^{-2} $s^{1/2}$ for W [29], only misalignments of the order of 0.3mm and above or high ELM loads might lead to local melting.

Evidently, the NBI heating upgrades [30] can potentially deliver more energy than the divertor can handle. It is mandatory that the physics scenarios are developed in such a way that they stay within the presented limits of power and energy deposition. An indispensable ingredient will be radiative cooling at the plasma edge [31]: radiative fractions of the order of $f_{rad} \approx 0.65$ may be

required to maintain adequate performance while keeping strike point loads within specifications [32]. Lastly, note that the maximum tolerable temperatures are reached for some specific components only minutes after the plasma pulse, which leaves little to no room for corrective actions during a discharge. It takes about 500s for the heat wave propagating downwards from the tile to the base carrier to reach the upper spring elements which are the more vulnerable ones. Strict observance of the prescribed temperature limits can only be fulfilled with the help of adequate look up tables and operating instructions - including the experimental knowledge of the initial boundary conditions -, as well as enough time to accommodate an appropriate learning curve, especially during re-start phases. The restart is stepwise with gradual increase of input power and plasma current starting from low power L-mode to high power H-mode in the first year of operation [3,4].

By way of a disclaimer, all values mentioned in the present article cannot be taken for granted from the beginning of tokamak operation. A thorough check is needed during the actual restart and early operation. On the experimental side, the boundary conditions which are the most important, for instance thermal contacts, may be significantly different. On the modelling side, the (experimental) validation of the calculations was limited and some parameters like material properties and, again, contact conditions had to be assumed from educated guesses; the situation in the torus may thus be fairly different.

CONCLUSIONS

All components in a metallic, inertially cooled divertor row may obviously suffer from excessive temperatures. The effective balance was slightly shifted in such a way that, except from cases of very localised loads, elements of the supporting structure come first close to the limits, that is before damage of the tungsten tile occurs. The reasons for this choice are the uncertainty on the actual properties of a production refractory material and the goals of the ITER-like Wall project to study the relevant combination of mixed materials, i.e. in the present case tungsten at the strike points. Tungsten remains vulnerable at both ends of the temperature domain of operation. So three temperature limits were specified in the first place, for the tungsten tile, the Inconel carrier and the clamping arrangement. They translate, albeit not straightforwardly, into admissible energy densities on the plasma wetted area.

The tile segmentation calls for a careful approach to extremely shallow angle(s) of incidence of the field lines because of either low wetted fractions or possible occurrence of leading edges. Experimental HHF tests under shallow angles proved quite valuable in this respect. The segmentation is also responsible for the impossibility to use the full amount of material for better cooling through side heat transfer. These limitations are of fundamental nature for an inertially cooled, segmented design. The design would exhibit an equal performance to CFC if the full bulk W tile area were utilisable but integrals of deposited power fall short due to segmentation and typical plasma footprints.

The bulk tungsten divertor row should help in investigating the adequacy of the material for plasma-facing components, in spite of the very specific boundary conditions (thermal insulation, inertial cooling) in JET.

ACKNOWLEDGEMENTS

Many thanks deserve all members of the "bulk W" team, an extensible group of five to one hundred technicians and scientists, depending on the current activities [33]. The author is particularly indebted to the late Contract Project Manager Henk Altmann who followed the bulk tungsten tile procurement right up to the installation with great commitment. He gave us in many occasions invaluable advice with high experience and professionalism. We are also grateful to G.F. Matthews, F. Romanelli and U. Samm who provided an adequate frame for the project to develop and proceed to a timely procurement. This work, supported by the European Communities under contracts between EURATOM and Forschungszentrum Jülich (Association), was carried out within the framework of the European Fusion Development Agreement (EFDA). The views and opinions expressed herein do not necessarily reflect those of the European Commission.

REFERENCES

[1]. Matthews G.F. *et al*., 2007 Physica Scripta **T128** 137
[2]. Riccardo V. *et al*., 2009 Physica Scripta **T138** 014033 (5pp)
[3]. Matthews G.F. *et al*., 2011 Physica Scripta, present topical issue
[4]. Brezinsek S. *et al*., 2011 Journal of Nuclear Materials in press (doi:10.1016/j.jnucmat.2010.10.037)
[5]. Maddison G. *et al*., 2011 Nuclear Fusion **51** 042001 (6pp)
[6]. Joffrin E. *et al*., 2010 Proc. 23rd IAEA Fusion Energy Conference, IAEA-CN-180/EXC/1-1
[7]. Rapp J. *et al*., 2009 Nuclear Fusion **49** 095012 (11pp)
[8]. Brezinsek S. *et al*., 2011 Nuclear Fusion, in press
[9]. Sadakov S. *et al*., 2007 Fusion Engineering and Design **82** 1825
[10]. Raffray A.R. *et al*., 2010 Fusion Engineering and Design **85** 93
[11]. Rieth M, Hoffmann A 2010 International Journal of Refractory Metals Hard Materials **28** 679
[12]. Greuner H. et al 2011 Journal of Nuclear Materials in press (doi:10.1016/j.jnucmat.2010.12.215)
[13]. Philipps V. 2011 Journal of Nuclear Materials in press (doi:10.1016/j.jnucmat.2011.01.110)
[14]. Neu R. *et al*., 2009 Physica Scripta **T138** 014038 (6pp)
[15]. Mertens Ph. *et al*., 2009 Fusion Engineering and Design **84** 1289
[16]. Mertens Ph. *et al*., 2009 Physica Scripta **T138** 014032 (5pp)
[17]. Mertens Ph. *et al*., 2011 Journal of Nuclear Materials in press (doi:10.1016/j.jnucmat.2011.01.113)
[18]. Nicolai D. *et al*., 2011 Fusion Engineering and Design accepted for publication
[19]. Rapp J, Pintsuk G and Mertens Ph 2010 Fusion Engineering and Design **85** 153
[20]. Jachmich S. 2010 private communication
[21]. Third Dimension, Bristol –UK, < http://www.third.com >
[22]. Mertens Ph. *et al*., 2011 Fusion Engineering and Design in press (doi:10.1016/j.fusengdes.2011.03.044)

[23]. Densamet® is the trademark of a tungsten alloy by MG Sanders Co Ltd, Stone –UK, member of the Rubicon Partners Group, < http://www.mgsanders.co.uk >
[24]. Hirai T. *et al*., 2007 Fusion Engineering and Design **82** 1839
[25]. Hirai T. *et al*., 2007 Physica Scripta **T138** 144
[26]. Neubauer O. *et al*., 2005 Fusion Science Technology **47** 76
[27]. Grigoriev S. *et al*., 2009 Fusion Engineering and Design **84** 853
[28]. Eich T. *et al*., 2011 Journal of Nuclear Materials in press (doi:10.1016/j.jnucmat.2010.11.079)
[29]. Pintsuk G, Kühnlein W, Linke J and Rödig M 2007 Fusion Engineering and Design **82** 1720
[30]. Ćirić D. *et al*., 2011 Fusion Eng. Des. in press (doi:10.1016/j.fusengdes.2010.11.035)
[31]. Giroud C. *et al*., 2010 Proc. 23rd IAEA Fusion Energy Conference, IAEA-CN-180/EXC/P3-02
[32]. Huber H. *et al*., 2011 Proc. 38th EPS Conference on plasma Physics, Strasbourg
[33]. see last section of the Final Report of the ILT Project (sect.11 available on demand)

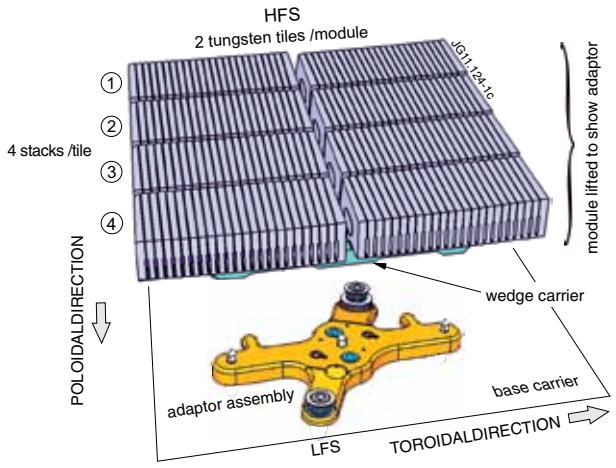

Figure 1: Full view of a bulk W module.

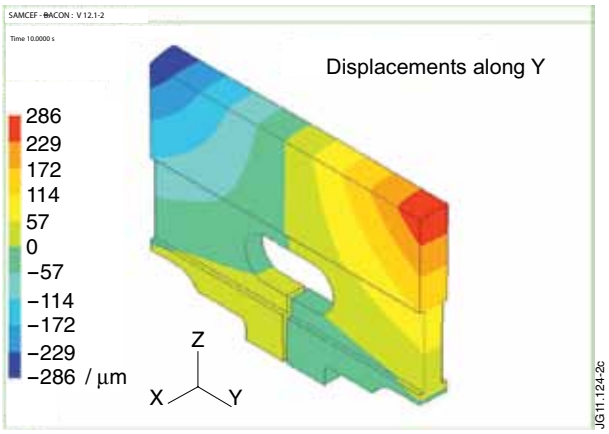

Figure 2: Thermal expansion of tungsten along the length in the lamella plane for the deposited energy which leads to $T_{Wsurf,max.}$ =2200°C.

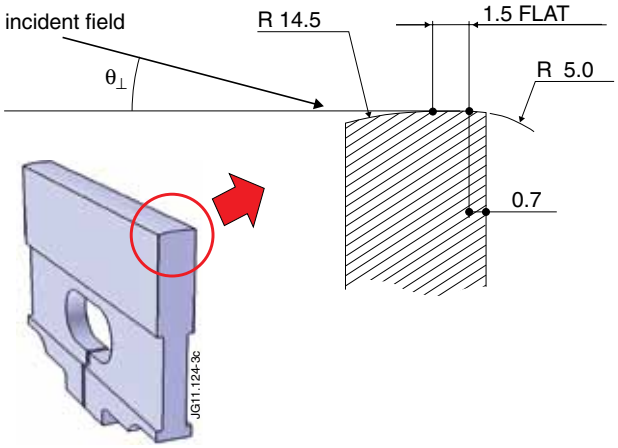

Figure 3: Two-dimensional profile of the plasma-facing surface of a lamella.

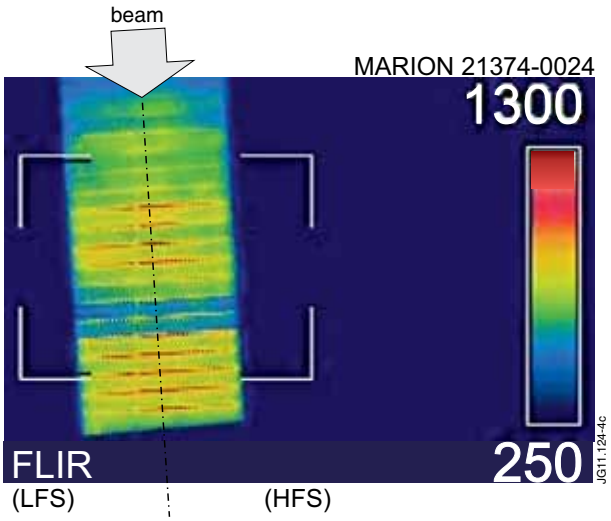

Figure 4: Infrared view of the plasma-facing surfaces.

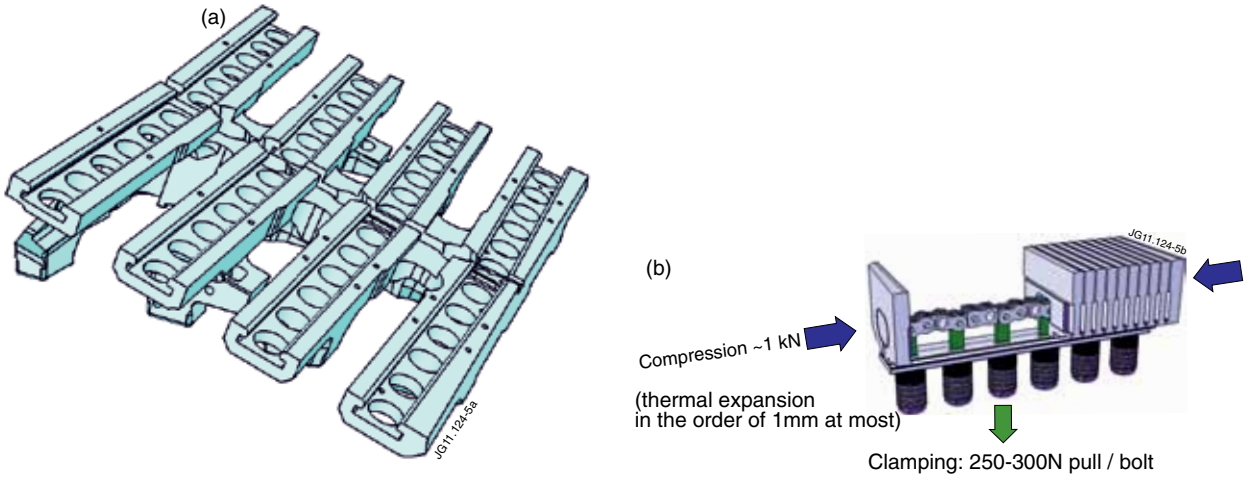

Figure 5: (a) Wedge carrier (b) Exploded view of the tile clamping.

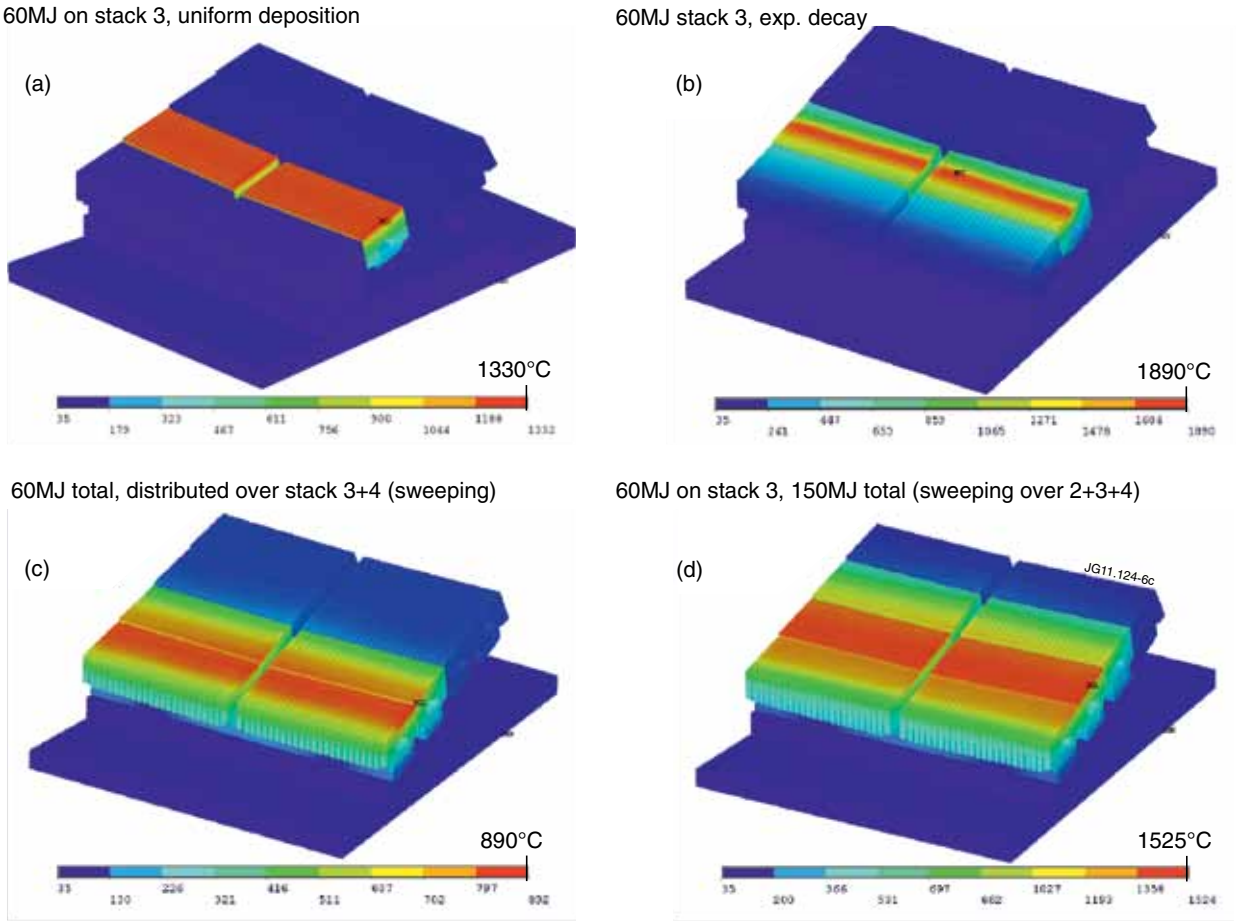

Figure 7: Finite element simulations of the heat transfer through a bulk W module: surface temperature of the tile following immediately a 10 s pulse with E_{dep}=60MJ/m^2, toroidal wetted fraction =1: a) uniform power deposition, b) account of exponentially decaying profiles (see text), c) still 60MJ in total, sweeping over stacks No. 3 and 4, d) 60MJ on stack 3, but 150MJ in total (swept over 2+3+4). The highest temperature on the tile surface is indicated in each case.

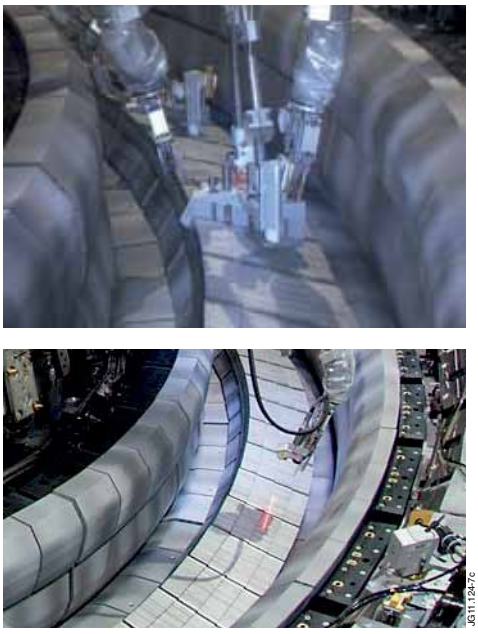

Figure 8: Remote Handling installation of the bulk W modules and subsequent Gap Gun survey